Slow relaxation of randomly packed hard spheres



2007 J. Phys.: Condens. Matter 19 356202

(http://iopscience.iop.org/0953-8984/19/35/356202)

IOP PUBLISHING JOURNAL OF PHYSICS: CONDENSED MATTER

J. Phys.: Condens. Matter **19** (2007) 356202 (11pp) doi:10.1088/0953-8984/19/35/356202

# Slow relaxation of randomly packed hard spheres

**Jongjin Lee[1], Changwon Lee[1], Insuk Yu[1], Youngkyun Jung[2] and Jysoo Lee[2]**

[1] School of Physics and Nano-Systems Institute (NSI-NCRC), Seoul National University, Seoul 151-747, Korea
[2] Supercomputing Center, Korea Institute of Science and Technology Information, PO Box 122, Yuseong-gu, Daejeon 305-806, Korea

E-mail: yjung@kisti.re.kr

Received 22 June 2007, in final form 26 June 2007
Published 1 August 2007
Online at stacks.iop.org/JPhysCM/19/356202

**Abstract**

We discover that the apparent weight and the electrical resistance of randomly packed stainless steel balls exhibit unusually slow relaxation behavior. It is found experimentally that these relaxations are due to structural change of the packing. Simultaneous measurements of the apparent weight and the electrical resistance show correlated time dependence. We have also performed two-dimensional molecular dynamics simulations and studied a possible mechanism for the slow relaxation behavior observed in experiments.

## 1. Introduction

The packing of grains under a series of weak mechanical perturbations shows interesting and unexpected features [1, 2]. Since Janssen demonstrated that the weight on the bottom of a container exponentially approaches a limit value as the column height increases [3, 4], many authors have extensively studied static packing [5–14]. The compaction dynamics to a steady state can be studied by the measurement of the packing density. Knight *et al* [11] first studied a density relaxation law in granular compaction and they observed that the relaxation can be well fitted by the inverse of the logarithm of the number of taps. But the boundary effect is very strong due to the small horizontal gap between the lateral walls used in their experiments. To avoid this effect, more recently, Philippe *et al* [12] carried out experiments with a larger horizontal gap and suggested that the relaxation is better fitted by a stretched exponential function. Another measurement of interest in studying compaction is the electrical resistance of conductive granular packing, which is very highly sensitive to an electrical perturbation [13, 14]. Vandewalle *et al* [15] measured the electrical resistance in a two-dimensional (2D) system under repeated tapping and found that the exponential function is in best agreement with their experiments. Such slow relaxation behavior can also be found in granular packing even when no external perturbation is submitted any more, after pouring

  

grains into a box. Two of us [16] have reported the slow relaxation of the electrical resistance of a static granular assembly of steel balls. Another experiment [17] also presented evidence of the relaxational changes of the electrical capacitance for a long time. However, in order to understand the origin of the slow relaxation in granular packing, it is necessary to know where such unusual behavior comes from.

In this paper, we experimentally study the relaxations of the physical quantities of granular packing after pouring stainless steel balls without any external perturbation: the apparent weight of the pile of balls that a weighting scale measures and the electrical resistance between electrodes attached to the side walls of the box. Both quantities show unusually long relaxation behavior. We find that there exist two distinctive stages in the relaxations and linear relations between the apparent weight and the electrical resistance. The relaxations in the early stage are fitted well to a stretched exponential function for a 3D packing and a double exponential function for a 2D packing. We also quantitatively analyze the characteristics of the two different relaxation stages by loading and unloading a weight on the top of the packing.

Two-dimensional molecular dynamics (MD) simulations have further been performed to study the source for the slow relaxation behavior observed in experiments. Investigations of the normal force at the bottom suggest that the slow relaxation is due to the structural relaxation of the packing induced by the isolated particles moving for a long time in the arches with nonzero kinetic energy.

## 2. Experiment

The scheme of experimental setup is shown in figure 1. From the preliminary study we found that the relaxation is very sensitive to room temperature change and external vibration [16]. Even a small change triggered new relaxations. The whole setup was placed in a doubly shielded box. We control the temperature inside the box actively by using a temperature controller (LakeShore 331). A temperature sensor (Pt 100 Ω) is positioned near the box. Four heaters are positioned at the sides of the anti-vibration table. We put thermal barriers in front of the heaters to prevent direct heating. By using these methods we can suppress the temperature fluctuation to less than 0.05 °C. During the experiments, the humidity is kept in the range $20 \pm 3\%$, whose influence is negligible in our experiments [18].

The rectangular box and its standing legs (thick lines in the figure 1) are made of aluminum plates of thickness 10 mm and 15 mm, respectively. For the electrical resistance measurement a 1 mm thick acryl plate and a commercial copper printed circuit board are attached to the inside facing wall of the box as an electrode. The voltage difference between two electrodes is measured using a sensitive voltmeter (Keithley 182) at opposite sides of the box while a constant current (1 mA) flows (Keithley 224). To keep the Joule heating minimal we turn on the current only when we need to measure voltage, but a continuous driving current does not make any difference.

In total, 17 000 stainless steel (type 316 with density $\rho = 8.03$ g cm$^{-3}$) balls of 3 mm diameter were used; they have strong resistance to oxidation. An electronic scale (Ohaus, ARD120) is used to measure the weight of the pile inside the box. The stabilization time constant of the scale is 3 s.

Before the start of experiment, the system is equilibrated at a desired temperature. The balls are then poured into a box through a hopper, the outlet of which is held at the same level as the opening of the box. The pouring time is about 5 s. Just after pouring ($t = 0$) we start to measure the apparent weight and the resistance of the balls, and the temperature of the system simultaneously.

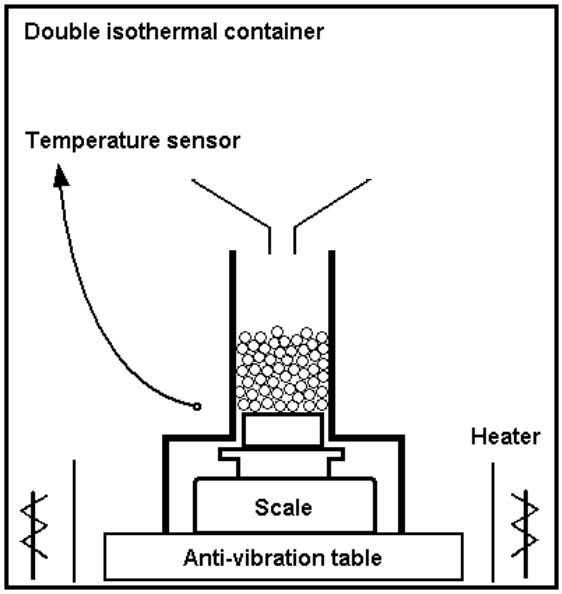


**Figure 1.** Experimental setup. Extensive shielding was used to minimize the temperature change and vibration. 3D (60 mm × 60 mm × 200 mm) and quasi-2D (5 mm × 60 mm × 200 mm) aluminum boxes were used. Stainless steel ball bearings (diameter 3 mm) were poured through a hopper. Two electrodes were attached on two opposite side walls of the box.

## 3. Results

### *3.1. Relaxations of 3D and 2D packing of balls*

We experimentally measured the apparent weight of poured balls acting on the bottom and the electrical resistance between two opposite sides of the box. Ten different experiments were performed in the same experimental conditions. Figure 2 shows the typical relaxations of them, normalized by the initial apparent weight (1627 g) and the initial resistance (10.5 Ω) measured just after pouring, respectively. Both of them show very slow relaxations lasting even up to a few tens of hours with two different regimes. In the early regime, the normalized electrical resistance decays faster than the normalized apparent weight; the situation is the opposite in the late regime. This will be explained later in detail.

The decrease of the electrical resistance is expected to be strongly associated with the apparent weight. In order to find the relations between them, we plot the normalized bottom weight as a function of the normalized electrical resistance as shown in figure 3. We can find somewhat linear relations between the relaxations of two quantities in the early stage of the experiment. Later, this linear relation breaks and fluctuates from sample to sample, which may depend on the different packing structures of the corresponding samples. We will call these two distinctive regimes the 'early' stage and the 'late' stage, respectively.

Since the early stage shows a systematic linear behavior independent of the trials of the experiment, we focus on the form of the relaxation of the apparent weight in the early stage. Figure 4 shows that a typical relaxation for a 3D packing is fitted well to a stretched exponential function

$$W_{3d}(t) = W(0) + \{W(\infty) - W(0)\}[1 - \exp(-(t/\tau_s)^{\alpha})], \quad (1)$$

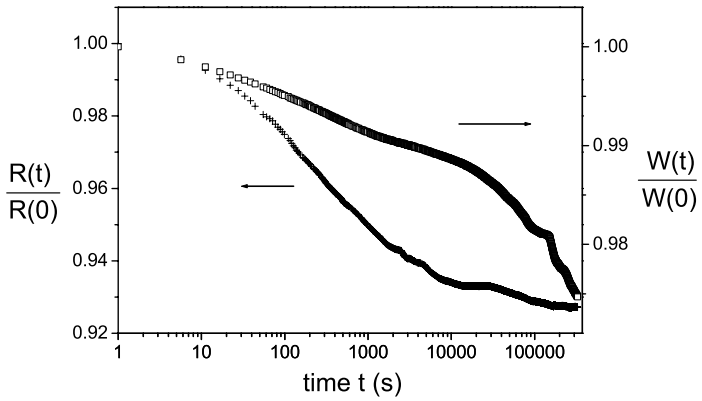


**Figure 2.** Slow relaxations of the 17 000 stainless steel balls in a 3D box. Just after pouring ($t = 0$) the measured apparent weight is $W(0) = 1627$ g (the actual weight is 2000 g) and resistance $R(0) = 10.5\ \Omega$. The weight (□) and resistance (+) are normalized to the values at the start of experiment.

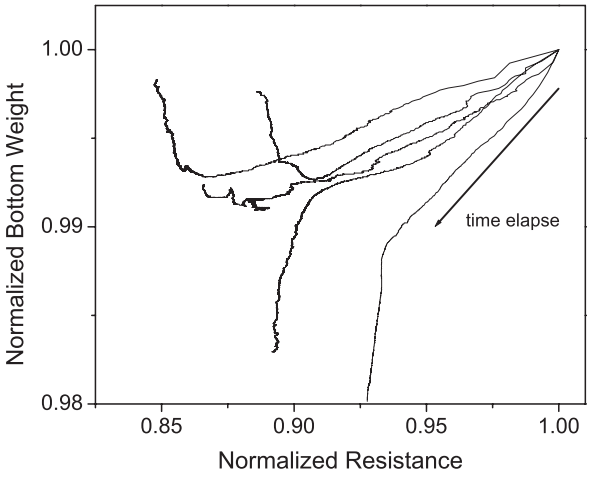


**Figure 3.** The normalized apparent weight and resistance show two distinctive time regimes: an initial linear regime and a largely scattered later regime. We call the first the 'early' stage and the latter the 'late' stage, respectively. The lowest graph corresponds to the data in figure 2. The arrow indicates the direction of time flow.

where $W(0)$ and $W(\infty)$ are the weights before and after the relaxation, respectively, $\tau_s$ a characteristic time constant, and $\alpha$ the control parameter. The $\tau_s$ and $\alpha$ values used in figure 4 are 256 s and 0.37, respectively.

We also performed quasi-two-dimensional experiments by reducing one side of the box to 5 mm and observed similar relaxation phenomena to those from the 3D experiments. Unlike in the 3D packing, the data for planar packing in figure 4 are well fitted to a double exponential function

$$W_{2d}(t) = W(0) + W_1 \exp(-t/\tau_1) + W_2 \exp(-t/\tau_2), \tag{2}$$

where $\tau_{1,2}$ are characteristic times and $W_{1,2}$ are constants. The two time constants used in figure 4 are 26 and 208 s.

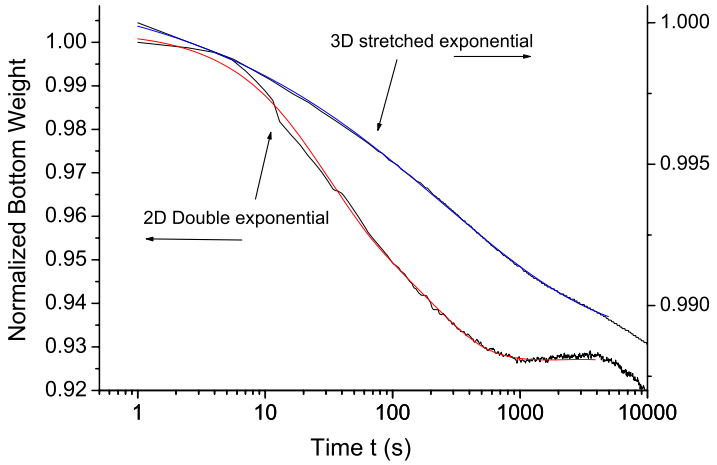


**Figure 4.** Early stage relaxation forms of the 3D and 2D packings: a stretched exponential form for 3D and a double exponential fitting to the majority of data for the 2D packings. The $\tau_s$ and $\alpha$ values in equation (1) for the 3D packing are 256 s and 0.37, respectively. The two time constants of the double exponential form in equation (2) for the 2D packing are 26 and 208 s.

(This figure is in colour only in the electronic version)

### *3.2. Response to a small mass load–unload*

To examine the characteristics of the two different relaxation stages we performed repeated small mass load–unload experiments at two different times: a few minutes after pouring ('early' stage) and after a few tens of hours at the end of the long time relaxation ('late' stage). The successive loading and unloading of a 73 g weight on the pile were performed at 15 s intervals.

When we first load a weight in the 'early' stage, the apparent weight of the balls abruptly increases, as shown in figure 5(a). But the amount of increase is only 2% of the loading (about 1.5 g compared with 73 g load). The rest of the load of the weight is screened by the pack of balls as the form of wall friction. The increased wall friction means an increase of the normal force to the side walls, which is revealed by the decrease in the lateral electrical resistance. It can be seen in figure 5 that the electrical resistance decreases as the apparent weight increases. When we unload the weight the apparent weight returns to its decaying value prior to the perturbation. Since the structure of the system and the networks of contact paths between the particles in this stage are still changing with time, the loading and unloading do not affect the overall relaxation procedures.

In the 'late' stage, all the quantities are pretty well relaxed already, unlike in the early stage, which is clearly observed in figure 5 (see the initial portion of each plot up to 70 s). When we load a small weight to the fully relaxed system both the apparent weight and the resistance increase with the first loading. After unloading, the apparent weight returns to the previous value with small fluctuation amplitude, but the resistance does not. During successive loading and unloading at 15 s intervals, the resistance still increases, unlike the apparent weight. This could be due to the small time interval between the loading and unloading. If the loading and unloading are performed at a long time interval so that the system reaches a stable state, the resistance will decrease after unloading, like the apparent weight. In this stage, since both quantities depend sensitively on the structure of the contact paths between the particles; the amplitudes of the decaying quantities will be different from one sample to another.

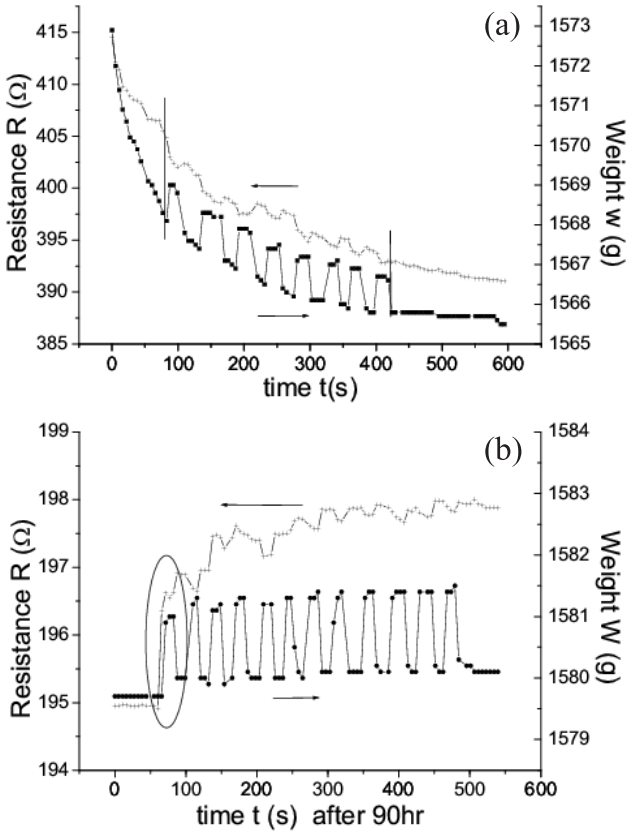


**Figure 5.** Repeated small mass load responses in (a) 'early' and (b) 'late' stages. 'Early' stage baselines are decreasing in both quantities with the load (a 73 g weight) applied. The 'late' stage shows a flat baseline before the application of load. For the first few loadings in the 'late' stage both quantities increase. We mark the time when the load of a small mass starts.

## 4. Simulations

### *4.1. Setup*

We model the system with two-dimensional molecular dynamics simulation and study the source for the slow relaxation of the normal force acting on the bottom which was observed in above experiments. The interaction between particles used in the present simulations is that of Cundall and Strack [19]. For an $N$ particle system, a particle can interact with any of the remaining $N-1$ particles. Let the coordinate of the center of particle $i(j)$ be $\vec{R}_i(\vec{R}_j)$, and $\vec{r} \equiv \vec{R}_i - \vec{R}_j$. In two dimensions, a new coordinate system defined by two vectors $\hat{n}$ (normal) and $\hat{s}$ (shear) will be used. Here $\hat{n} = \vec{r}/|\vec{r}|$, and $\hat{s}$ is defined as rotating $\hat{n}$ clockwise by $\pi/2$. The force between two particles in contact with each other can be decomposed into the normal component $F_\mathrm{n}$ and the shear component $F_\mathrm{s}$. With a relative normal compression $\Delta = (a_i + a_j - |\vec{r}|)$, the components of the force acting on particle $i$ by particle $j$ are given as

$$F_\mathrm{n} = k_\mathrm{n}\Delta^{1+\beta} - \gamma_\mathrm{n} m_\mathrm{e}\Delta^{\kappa}(\vec{v}\cdot\hat{n}), \tag{3}$$

and

$$F_\mathrm{s} = -\,\mathrm{sgn}(\delta s)\,\min(k_\mathrm{s}|\delta s|, \mu|F_\mathrm{n}|) - \gamma_\mathrm{s} m_\mathrm{e}(\vec{v}\cdot\hat{s}), \tag{4}$$

where $a_i(a_j)$ is the radius of particle $i(j)$, $\vec{v} = \mathrm{d}\vec{r}/\mathrm{d}t$, and $m_\mathrm{e} = m_i m_j/(m_i + m_j)$. $\beta = \kappa = 0$ for Hookean (linear) contacts, while for Hertz–Kuwabara–Kono (nonlinear) contacts $\beta = \kappa = 1/2$ [20]. The first term in equation (3) is an elastic force, and the second is a velocity-dependent damping term. Here $k_\mathrm{n}$ is the normal elastic constant, and $\gamma_\mathrm{n}$ is the damping coefficient. Static friction is implemented in equation (4). Given total shear displacement $\delta s$ during a contact, a restoring force with elastic constant $k_\mathrm{s}$ is created, and $\mu$ is the friction coefficient. The second term in equation (4) is a velocity-dependent damping term. A particle also can interact with a wall. The force on particle $i$ in contact with a wall is given by equations (3) and (4) with $a_j = 0$ and $m_\mathrm{e} = m_i$. For more details of the interaction, please see [21].

For the linear model ($\beta = \kappa = 0$), the parameters used are $k_\mathrm{n} = 10^6$ g s$^{-2}$, $k_\mathrm{s} = 10^6$ g s$^{-2}$, $\gamma_\mathrm{n} = 5.0 \times 10^4$ s$^{-1}$, $\gamma_\mathrm{s} = 0.0$ s$^{-1}$ and $\mu = 0.2$. The timestep is taken to be $7.9 \times 10^{-7}$ s. For the nonlinear model ($\beta = \kappa = 1/2$), we set $k_\mathrm{n} = 1.4 \times 10^7$ g s$^{-2}$, $k_\mathrm{s} = 10^7$ g s$^{-2}$, $\gamma_\mathrm{n} = 2.5 \times 10^6$ s$^{-1}$, $\gamma_\mathrm{s} = 1.6 \times 10^5$ s$^{-1}$, and the timestep is $5.0 \times 10^{-8}$ s. Particles with mean diameter 0.02 cm are used. The particles are polydisperse, and their diameters are drawn from a Gaussian whose width is 10% of its mean. The material density of particles is 5.0 g cm$^{-3}$. CGS units are implied throughout the paper.

Simulations are started by putting $N$ particles in a close-packed configuration in a two-dimensional box of width $W$ and height $H$, instead of pouring the particles into the box. Initially, the particles fall and gain kinetic energy due to gravity; they lose it by dissipation. A fixed boundary condition is used. Simulations were performed with $N = 1250$, $W/D = 25$, and $H/D = 50$, where $D$ is the mean particle diameter. To see more long-time behavior, we also performed simulations with $N = 625$ and $W/D = 25$.

### *4.2. Results*

We first measure the normal force acting on the bottom of the box. We initially would expect that a stable packing structure is revealed after a short transient. However, the normal forces for the linear model (left three figures) as well as for the nonlinear one (right three figures) in figure 6 reveal several cases of the long-time slow relaxations, which are well consistent with the experimental observations. For the linear case, the normal forces increase or decrease in a stepwise manner depending on the corresponding packing structure. The stepwise relaxation may come from the fact that the response to some perturbation disappears rapidly due to larger dissipation.

In order to gain an insight into such an unusual slow relaxation, we study the normal force networks of the granular packing. Figure 7 shows the force networks which are taken at two different time indicated by arrows (1) and (2) in figure 6, where there are sudden decreases in the normal force. We can hardly find significant differences in the force networks as well as the packing structures. The only difference is the position of a particle indicated by arrows in figure 7 which is in contact with the bottom and isolated in an arch. A possible scenario of the long-time slow relaxation is for isolated particle in an arch to move freely with nonzero kinetic energy which is gained due to gravity. Collision of an isolated particle with its neighbor can change the contact networks partially between the particles and induce the redirection of the force field.

To be sure, we keep track of an isolated particle moving with nonzero kinetic energy. After collision with its neighbor, the velocity of the isolated particle decreases due to dissipation and its sign is changed, as shown in figure 8. The time of a change in the particle velocity is exactly in accordance with that of a sudden change in the normal force acting on the bottom. From this fact, we expect that an isolated particle with nonzero kinetic energy plays a key role in the slow relaxation of the system.

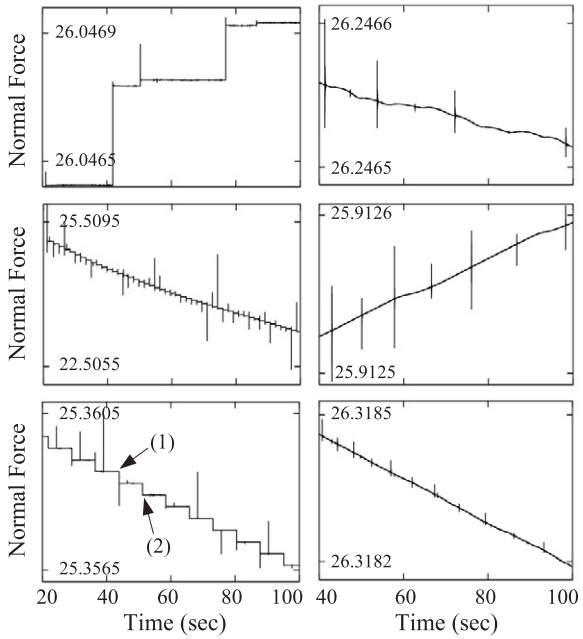


**Figure 6.** Slow relaxation of the normal force on the bottom of the box for the linear model (left three figures) and the nonlinear one (right three figures). The unit of the normal force is g cm $s^{-2}$.

To make sure of the role of the isolated particle, we next measure the difference of the normal forces between successive timesteps. Figure 9 shows the time evolution of the force difference after an isolated particle collides with its neighbor. Figure shows that an isolated particle with nonzero kinetic energy plays a role as a initiator of the slow relaxation. After colliding with its neighbor, the isolated particle transmits its kinetic energy to the neighbor particle and loses it by dissipation. The collisions with the neighbors by avalanche can spread throughout the system and they give rise to the changes of the normal forces between the particles.

We have also performed simulations for the nonlinear contacts. In this case, due to less dissipation with lower particle velocity [22], the kinetic energy loss occurs more slowly than that for the linear model. This thus induces a continuous change of the normal force, unlike the stepwise relaxation in the linear model, as shown in figure 6. Apart from this difference in relaxation, there is no any difference between two models.

### *4.3. Discussions*

Even though the perturbation is very small, it can affect the packing structure in a granular system and induce the slow relaxation to a stable state. Our observations in simulations suggest that the long-time slow relaxation of the normal force on the bottom of a box results from isolated particles moving with nonzero kinetic energy; these particles are in contact with the bottom and isolated in arches. The isolated particles do not exist in the bulk, but on the bottom, and their number is few. After a few seconds of relaxation, all the particles except the isolated particles are packed tightly together, so they can hardly move. However, even though there exists only one isolated particle with nonzero kinetic energy, relaxation occurs, as shown in figure 9. In the case that the isolated particles lose their energy due to the dissipation,

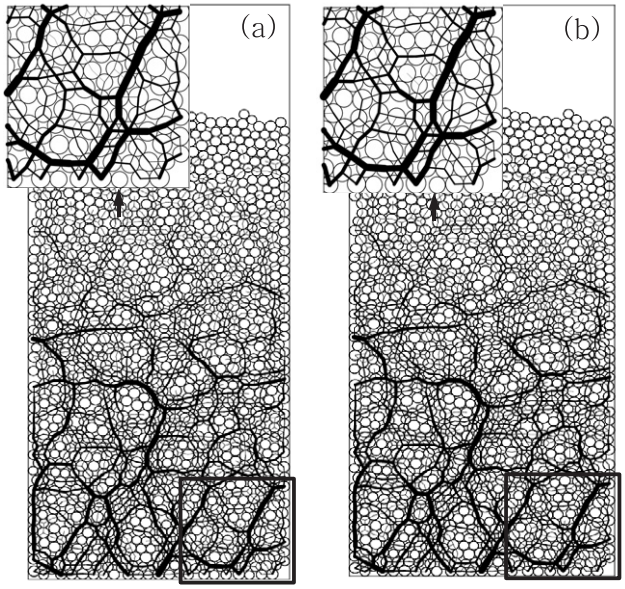


**Figure 7.** Networks of the normal force which are taken at two different times indicated by arrows (1) and (2) in figure 6. An isolated particle collides with a left neighbor (left) and a right neighbor (right), respectively. It is hard to find a difference in the normal force networks between two figures except for the positions of two isolated particles indicated by arrows. Different width of interconnecting segments denotes the different interparticle normal force. The portions in the small boxes are enlarged so that the individual particles can be seen clearly.

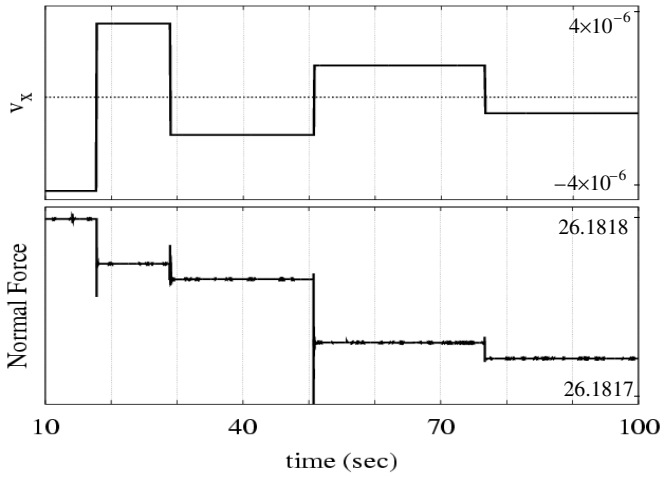


**Figure 8.** Horizontal velocity $v_x$ of an isolated particle and the normal force on the bottom as a function of time. Whenever the sign of the velocity changes, there exist changes of the normal force. The horizontal dotted line denotes the zero of the horizontal velocity. Units of the velocity and the normal force are cm $s^{-1}$ and g cm $s^{-2}$, respectively.

relaxation does not occur. Although it is difficult to find such behavior of the isolated particles in experiments, it can be expected that the particles have some kinetic energy for a long time in experiments, even though it is a very small amount, so relaxation occurs. Our studies suggest

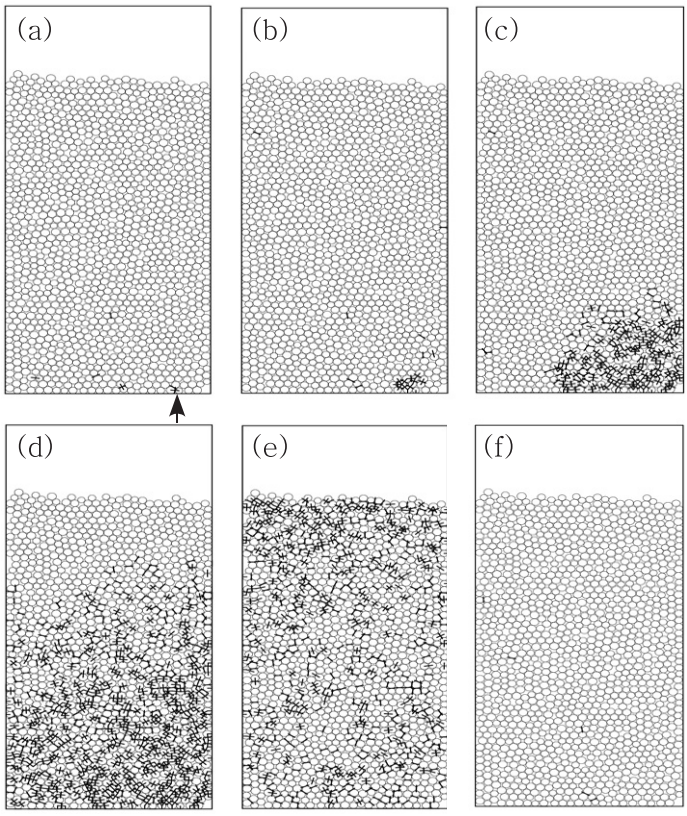


**Figure 9.** Time evolution of the difference of the normal forces between successive timesteps after an isolated particle collides with a neighbor (from (a) to (f)). After collision, there exists a change of the normal force which spreads throughout the system and disappears. The interconnecting segments among the particles denote the presence of the difference of the normal forces between successive timesteps.

a possible mechanism for the slow relaxation. However, more study is necessary to better establish the mechanism for the unusually slow relaxation shown in experiments.

## 5. Conclusion

We have observed the long-time slow relaxation of both the apparent weight and the electrical resistance in the packing of stainless steel balls confined in a container. The relaxation behavior appears up to a few tens of hours in our experiments. Simultaneous decreases in both quantities showed that these relaxations are caused by the redirection of force field from vertical to horizontal directions toward the side walls.

In experiments, we found two distinctive regimes of 'early' and 'late' stages in the relaxations. In the 'early' stage, the weight and the resistance have linear relations and the relaxations are well fitted to a stretched exponential function for a 3D packing and a double exponential function for a 2D case. In contrast, the 'late' stage has no distinctive relation between the two quantities.

Although these two stages could not be found in simulations, the slow relaxation of the normal force on the bottom was also found. We found that isolated particles with kinetic energy are responsible for the long-time relaxation of the granular packing.

## Acknowledgments

One of the authors (IY) acknowledges support from the Nano-Systems Institute (NSI-NCRC) program sponsored by the Korea Science and Engineering Foundation (KOSEF). This work was supported in part by a research fund from IBM Korea.

## References

[1] Herrmann H J, Hovi J P and Luding S (ed) 1998 *Physics of Dry Granular Media* (Dordrecht: Kluwer)
[2] de Gennes P G 1999 *Rev. Mod. Phys.* **71** S374
[3] Janssen H A and Vereins Z 1895 *Deutsch. Ing.* **39** 1045
[4] Boutreux T, Raphaël E and de Gennes P G 1997 *Phys. Rev.* E **55** 5739
[5] Bouchaud J P, Cates M E and Claudin P 1995 *J. Physique* I **5** 639
[6] Mueth D M, Jaeger H M and Nagel S R 1998 *Phys. Rev.* E **57** 3164
[7] Vanel L and Clément E 1999 *Eur. Phys. J.* B **11** 525
[8] Vanel L, Claudin P, Bouchaud J P, Cates M E, Clément E and Wittmer J P 2000 *Phys. Rev. Lett.* **84** 1439
[9] Bertho Y, Giorgiutti-Dauphiné F and Hulin J P 2003 *Phys. Rev. Lett.* **90** 144301
[10] Claudin P and Bouchaud J P 1997 *Phys. Rev. Lett.* **78** 231
[11] Knight J B, Fandrich C G, Lau C N, Jaeger H M and Nagel S R 1995 *Phys. Rev.* E **51** 3957
[12] Philippe P and Bideau D 2003 *Phys. Rev. Lett.* **91** 104302
Philippe P and Bideau D 2002 *Europhys. Lett.* **60** 677
[13] Branly E 1890 *C.R. Acad. Sci. Paris* **111** 785
[14] Guyon E 2002 *Pour la Science* **300** 130
[15] Vandewalle N, Lenaerts C and Dorbolo S 2002 *Physica* A **311** 307
[16] Yoon S S, Lee J J and Yu I 1999 *J. Korean Phys. Soc.* **35** S1326
[17] Massalska-Arodź M, Mayer J, Brańkowski J, Ostrowicz A and Lisiecki E 1997 *Phys. Rev.* E **55** 1225
[18] Bocquet L, Charlaix E, Ciliberto S and Crassous J 1998 *Nature* **396** 735
[19] Cundall P A and Strack O D L 1979 *Géotechnique* **29** 47
[20] Kuwabara G and Kono K 1987 *Japan. J. Appl. Phys.* **26** 1230
[21] Lee J and Herrmann H J 1993 *J. Phys. A: Math. Gen.* **26** 373
[22] Luding S, Clément E, Rajchenbach J and Duran J 1994 *Phys. Rev.* E **50** 4113